Industrial Engineering Journal
ISSN: 0970-2555
Volume : 52, Issue 11, No. 2, November : 2023

A SIMULATION STUDY OF TWO-LAYER DOUBLE PEROVSKITE SOLAR CELL EFFECT OF DEFECT AND WIDTH VARIATION ON PSC PARAMETERS TO OBTAIN OPTIMIZED PCE WITH MINIMUM WIDTH

Nishi Bala, Assistant Professor, Department of Electrical and Electronics Engineering, Bakhtiyarpur College of Engineering, Champapur, Dedaur, Bakhtiyarpur, Bihar, India E-mail: nishijnct@gmail.com
Abhishek Raj Research Scholar, Department of Mechanical Engineering, National Institute of Technology, Adityapur, Jamshedpur, Jharkhand, India 17araj@gmail.com

ABSTRACT: -
In this study, Comparison of inverted structure of two doubly layered Perovskite Solar Cell is investigated. The effect of width variation of different absorber layers with different parameters has been investigated to obtain optimum solar cell parameters like FF, Voc, Isc and PCE. Comprehensive simulation approach has been utilized using SCAPS-1D software. The major objective of present study is to analyze different defect density and thickness value of perovskite absorption layer for achieving the optimized parameter like PCE with the help of SCAPS-1D. The proposed device structure utilized CuSCN as a hole transport layer (HTL) and TiO_2 as an electron transport layer (ETL), $MA_3Sb_2I_9$ and $Cs_2AgBiBr_6$ as perovskite absorption layer (PAL), Indium tin oxide (ITO) as top electrode and Au as back contact. The simulation result shows that at the thickness of 200 nm of $Cs_2AgBiBr_6$ and 100 nm of $MA_3Sb_2I_9$ of defect density of 1×10^{14} cm^{-3} of PAL, the optimized parameters obtained are PCE 27.87%, Voc 1.04 V, Jsc 23.48 mA/cm^2 and fill factor (FF) 80.37%. The optimization of thickness of the double layered absorber materials in combination with reduced defect density provided a superior power conversion efficiency (PCE), much greater than the earlier reported values when $MA_3Sb_2I_9$ and $Cs_2AgBiBr_6$ were taken individually as the absorber layers.

Abbreviation: ITO –
Indium Tin Oxide, PSC- Perovskite Solar Cell, ETL-Electron Transport Layer, PCE – Power Conversion Efficiency, HTL-Hole Transport Layer, FF- Fill Factor

1. Introduction

PSC has emerged as a revolutionary and highly favorable technology in the field of photovoltaics. These innovative solar cells are named after the mineral perovskite, which has a crystal structure that inspired the design of the photovoltaic materials [1]. PSC offer a compelling alternative to traditional silicon-based solar panels, thanks to their remarkable efficiency, cost-effectiveness, and versatility [2-3]. These solar cells are a type of thin-film solar technology that has shown remarkable progress in a relatively short period. PSC are typically composed of a perovskite-structured compound as the light-absorbing layer. Perovskite solar cells' remarkable power conversion efficiency is one of their key benefits. Since their introduction, researchers have achieved efficiencies comparable to traditional silicon solar cells, with the potential for even higher performance [4-6]. This high efficiency is due to their excellent light-absorbing properties and efficient charge carrier transport. Perovskite solar cells offer the advantage of a relatively simple and low-cost fabrication process [7]. The materials used are abundant and inexpensive, contributing to the potential for cost-effective large-scale production. However, challenges related to stability and scalability still need to be addressed for commercial viability. Despite their rapid progress, PSCs face challenges, particularly in terms of long-term performance and stability [8-10]. Researchers are actively working to address issues related to material degradation, sensitivity to moisture, and the development of more reliable encapsulation techniques.
$Cs_2AgBiBr_6$ is a specific type of perovskite material. It is a double perovskite compound consisting of

bromine (Br), bismuth (Bi), silver (Ag) and cesium (Cs) elements. $Cs_2AgBiBr_6$ exhibits some intriguing characteristics that make it a subject of research. $Cs_2AgBiBr_6$ perovskite has a direct bandgap, which is highly desirable for solar cell applications [11-14]. Cs2AgBiBr6 exhibits favorable optical properties for solar absorption. Its bandgap can be tuned to absorb sunlight effectively, allowing for efficient conversion of solar energy into electricity. The electronic structure of Cs2AgBiBr6 allows for efficient charge carrier transport, which is important for attaining high power conversion efficiency in solar cells [15]. This means that it efficiently absorbs and converts a broad range of sunlight into electricity. Its bandgap can be tuned, making it adaptable for various solar spectrum conditions.

$MA_3Sb_2I_9$ is a perovskite material compound consists of metal (M), antimony (Sb), and iodine (I) elements, where M typically represents a combination of cesium (Cs) and methylammonium (CH3NH3 or MA). The inclusion of antimony (Sb) in the perovskite structure may contribute to specific electronic and optical properties [16-17]. Methylammonium cations are commonly used in PCSs due to their ability to form stable perovskite structures. $MA_3Sb_2I_9$ exhibits relatively good stability against moisture and oxygen compared to some other perovskite materials. Like many perovskite materials, $MA_3Sb_2I_9$ allows for the adjustment of its bandgap, which can be tuned to optimize solar absorption and enhance the overall performance of the solar cell [18]. This enhanced stability is a sought-after trait in the development of durable and long-lasting solar cells.

The present study objective is to evaluate the effect of factors namely width and defect density of perovskite absorption layer on the performance of n-i-p structure of PSC $ITO/TiO_2/MA_3Sb_2I_9/Cs_2AgBiBr_6/CuSCN/Au$, and p-i-n structure of PSC $ITO/CuSCN/MA_3Sb_2I_9/Cs_2AgBiBr_6/TiO_2/Au$ is investigated and simulated using SCAPS-1D software. Standard deep energy defect level of 0.6 eV is considered for the current study. We have utilized TiO_2 as ETL due of its stability and suitable band alignment. Double layered perovskite is considered as absorber layers. As HTL, CuSCN is used by facilitating the movement of positively charged "holes" created in the perovskite layers during the absorption of light. It helps in preventing the recombination of charge carriers and ensures efficient collection of holes for electrical current. [31]. For the suggested PSC structure, basic characteristics such as V_{OC},J_{SC}, PCE and FF were examined. The device modelling and illustration of result of different parameter requires software simulation and numerical modelling. The Solar Cell Capacitance Simulator (SCAPS) application used for this purpose.

This paper contains four sections. In Section 1 introduction of PSC devices and the materials taken for the proposed device are discussed in detail. In the section 2 proposed device structure and it's inverted structure is introduced, its schematic diagram, energy band diagram and the carrier transport mechanism inside device has been explained. In the section 3, various result of solar cell parameter that obtained by varying defect densities, width of $MA_3Sb_2I_9$ and $Cs_2AgBiBr_6$, Defect energy levels and Interface defect densities has been discussed. Optimum result of PCE obtained on a specific design parameter has been discussed and its comparison with previous works has been done. In the section 4, Conclusions have been provided and future works recommended for further enhancement of PCE and other solar cell parameter.

2. Proposed device architecture

An organic-inorganic PSC having a configuration $ITO/TiO_2/MA_3Sb_2I_9/Cs_2AgBiBr_6/CuSCN/Au$. The Proposed PSC device is shown in Fig. 1(a) and Fig. 1(b) shows $ITO/CuSCN/MA_3Sb_2I_9/Cs_2AgBiBr_6/TiO_2/Au$ the inverted structure. It is constructed using ITO, which works as a top electrode of 200 nm thickness. $MA_3Sb_2I_9$ as PAL 1 of thickness 100 nm, $Cs_2AgBiBr_6$ as PAL 2 of 200 nm thickness, TiO_2 as an ETL of width 40 nm, CuSCN as a HTL of width 50 nm. Au works as the back contact. Fig. 1(c) represent the working mechanism in the device, $MA_3Sb_2I_9$ captures solar spectrum photons whose energy is more than its bandgap of 1.53 eV and generate electron and hole pairs in the conduction and valance band of $MA_3Sb_2I_9$ then it passes to $Cs_2AgBiBr_6$ whose bandgap is

Industrial Engineering Journal
ISSN: 0970-2555
Volume : 52, Issue 11, No. 2, November : 2023

1.7 eV and it absorbs photons of energy level more than the bandgap of $Cs_2AgBiBr_6$. Generated Holes and Electrons move towards HTL and ETL respectively.

Figure 1(a) shows structural diagram of PSC device n-i-p structure, Figure 1(b) shows structural diagram of PSC device p-i-n structure and Figure 1(c) demonstrate energy band diagram and the carrier transport mechanism in proposed structure. Table 1 mention the used simulation parameters and material properties in this paper of $MA_3Sb_2I_9$ and $Cs_2AgBiBr_6$ based PSC device.

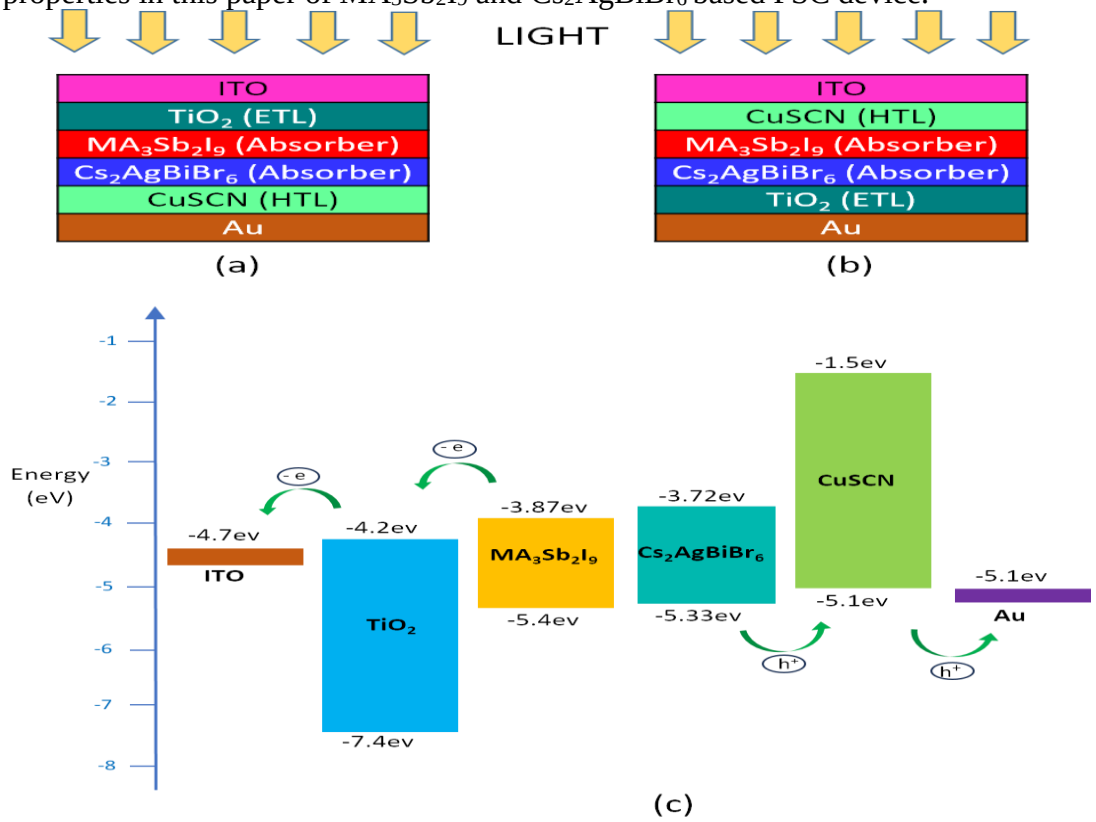

Fig. 1 (a) structural diagram of proposed PSC device (b) structural diagram of inverted PSC device (c) Energy band diagram and the carrier transport mechanism in $MA_3Sb_2I_9$ and $Cs_2AgBiBr_6$ based PSC device.

Fig. 1(c) shows band diagram with respect to vacuum level. Valence band and conduction band of sandwiched layers are compatible such that it allows smooth carrier transport. Electron and hole pair generate in perovskite absorption layer $MA_3Sb_2I_9$ and $Cs_2AgBiBr_6$, electron moves in conduction band of $MA_3Sb_2I_9$ of energy level -3.87 eV to ETL energy level -4.2 eV and further collected at ITO at energy level -4.7 eV. In this way electron moves from higher energy level to comparatively lower energy level to contribute current. Hole moves in valence band of $Cs_2AgBiBr_6$ of energy level -5.33 eV to HTL energy level at -5.1 eV and further collected at electrode Au at energy level -5.1 eV. Here hole moves in valence band lower energy level to comparatively higher energy level to contribute current. Similarly, in the inverted structure, Electron moves in conduction band of $Cs_2AgBiBr_6$ of energy level -3.72 eV to ETL energy level -4.2 eV and further collected at Au at energy level -5.1 eV. In this way electron moves from higher energy level to comparatively lower energy level to contribute current. Hole moves in valence band of $MA_3Sb_2I_9$ of energy level -5.4 eV to HTL energy level at -5.1 eV and further collected at ITO at energy level -4.7 eV.

Table 1 The properties of materials and simulation parameters in $MA_3Sb_2I_9$ and $Cs_2AgBiBr_6$ based PSC device

Parameters	CuSCN	$MA_3Sb_2I_9$	$Cs_2AgBiBr_6$	TiO_2	ITO
Thickness (nm)	50	100	200	40	200

Industrial Engineering Journal
ISSN: 0970-2555
Volume : 52, Issue 11, No. 2, November : 2023

E_g(eV)	3.17[21]	1.53[19]	1.7[20]	3.2[22]	3.5[22]
Electron Affinity (eV)	2.45[21]	3.87[19]	4.19	3.9	4[22]
Relative permittivity	3[21]	6.32[19]	5.8[20]	9[22]	9[22]
Conduction band effective density of states$N_c(cm^{-3})$	2.2×10^{18}[21]	1×10^{19}	1×10^{19}	1×10^{21}	2.2×10^{18}
Effective density and valence band of states$N_v(cm^{-3})$	1.9×10^{19}[21]	1×10^{19}	1×10^{19}[20]	2×10^{20}	1.8×10^{19}[22]
Electron thermal velocity (cm/s)	1×10^{7}	1×10^{7}	1×10^{7}	1×10^{7}	1×10^{7}[22]
Hole thermal velocity (cm/s)	1×10^{7}	1×10^{7}	1×10^{7}	1×10^{7}	1×10^{7}
Mobility of electron μ_e (cm^2/Vs)	2×10^{-4}[21]	6×10^{-4}[19]	9.28	20	20
Mobility of hole μ_h (cm^2/Vs)	2×10^{-4}	6×10^{-4}[19]	9.28	10	10
Donor density $N_D(cm^{-2})$	0	1×10^{18}	1×10^{16}	2×10^{19}	1×10^{21}
Acceptor density $N_A(cm^{-2})$	1×10^{18}	1×10^{18}	1×10^{16}	0	0
$N_t(cm^{-3})$	1×10^{14}	1×10^{14}	1×10^{14}	1×10^{15}	1×10^{15}

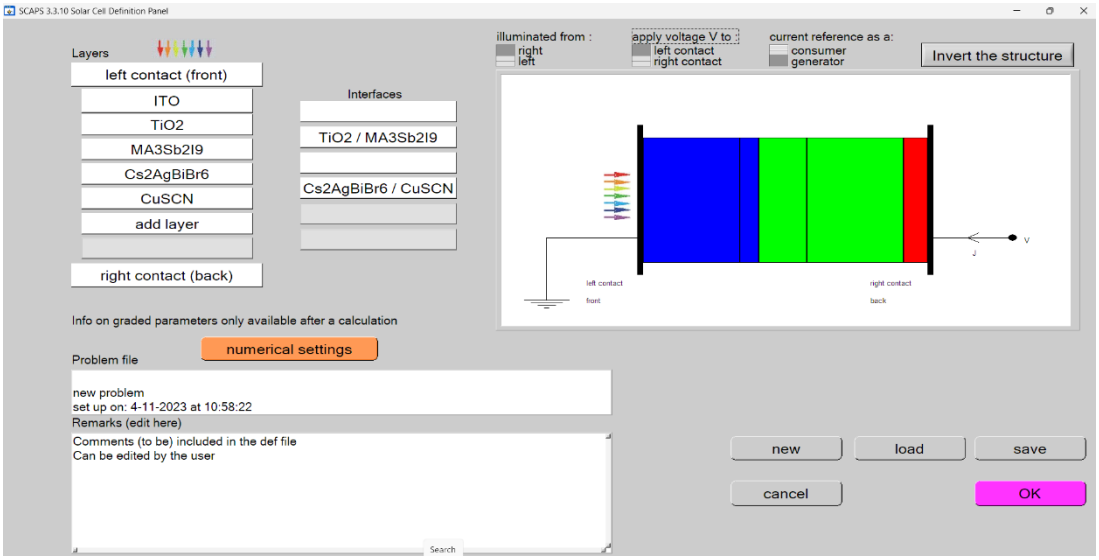

Fig. 2 Picture of SCAPS 3.3.10 Definition Panel containing the proposed structure.

3. Results and discussions

The effect of variation of defect density and thickness of the PAL, i. e. $MA_3Sb_2I_9$ and $Cs_2AgBiBr_6$ on the PSC device has been investigated to obtain specific PSC device which provide maximum PCE. Further, VI characteristics of the proposed layers ITO/TiO_2/$MA_3Sb_2I_9$ /$Cs_2AgBiBr_6$/CuSCN/Au and ITO/CuSCN/$MA_3Sb_2I_9$ /$Cs_2AgBiBr_6$/TiO_2/Au has been obtained and discussed. Standard deep energy defect level of 0.6 eV is considered. Effect of variation of series resistance, shunt resistance and temperature on V_{OC} , J_{SC} , FF and PCE is drawn and optimized result has been discussed.

3.1. Effect of $MA_3Sb_2I_9$ and $Cs_2AgBiBr_6$ thickness and Defect Density variations on PSC parameters

Industrial Engineering Journal
ISSN: 0970-2555
Volume : 52, Issue 11, No. 2, November : 2023

The simulation of $MA_3Sb_2I_9$ and $Cs_2AgBiBr_6$ based device is established by utilizing the parameters listed in Table 1. Effect of variation of defect density of $MA_3Sb_2I_9$ and $Cs_2AgBiBr_6$ is studied. Effect of variation of $MA_3Sb_2I_9$ and $Cs_2AgBiBr_6$ thickness at the defect density of 1×10^{14} cm^{-3} is investigated. Variation of V_{OC} , J_{SC} , FF and PCE with the defect density of $MA_3Sb_2I_9$ and $Cs_2AgBiBr_6$ is studied as it is varied from 1×10^{13} cm^{-3} to 1×10^{17} cm^{-3}. It is seen that V_{OC} decreases drastically as the defect density is increased from 1×10^{13} cm^{-3} to 1×10^{17} cm^{-3}. J_{SC} remains constant when defect density is decreased from 1×10^{13} cm^{-3} to 1×10^{14} cm^{-3} and it decreases when defect density is increased to 1×10^{17} cm^{-3}. FF also remains constant when defect density is decreased from 1×10^{13} cm^{-3} to 1×10^{14} cm^{-3} and it decreases when defect density is increased to 1×10^{17} cm^{-3}. PCE decreases 43% as the defect density is increased from 1×10^{13} cm^{-3} to 1×10^{17} cm^{-3}. Variation of FF, J_{SC}, V_{OC} and PCE with respect to change of thickness from 50 nm to 250 nm of $MA_3Sb_2I_9$ and 100 nm to 300 nm of $Cs_2AgBiBr_6$ is studied. It is well observed that V_{OC} continuously decreases with increase of $MA_3Sb_2I_9$ thickness, provides a maximum value 1.18 V which obtained at the $MA_3Sb_2I_9$ width of 50 nm. This may be explained as increase in $MA_3Sb_2I_9$ thickness allow absorption of more solar photon, results into increased charge carrier pairs. It is observed that J_{sc} increases with the thickness variation of $MA_3Sb_2I_9$ from 50 nm to 100 nm then it gradually reduces with the width increasing from 100 nm to 250 nm. It happened mainly due to increased rate of recombination. FF continuously decreased with the increasing $MA_3Sb_2I_9$ thickness, at 250 nm we obtained FF of 62.6% . FF reduce with increase of width from 50 nm to 250 nm. The PCE is increased till the thickness of $MA_3Sb_2I_9$ reached 100 nm then it continuously decrease with increase of $MA_3Sb_2I_9$ width from 100 nm to 250 nm, mainly due to decreased current density. Maximum PCE of 27.87% is obtained at 100 nm. V_{OC} continuously decreases with increase of $Cs_2AgBiBr_6$ thickness increases from 100 nm to 300 nm. J_{sc} remains constant with the thickness variation of $Cs_2AgBiBr_6$ from 100 nm to 200 nm and then it decreases as $Cs_2AgBiBr_6$ thickness increases from 200 nm to 300 nm. FF also remains constant with the thickness variation of $Cs_2AgBiBr_6$ from 100 nm to 200 nm and then it decreases as $Cs_2AgBiBr_6$ thickness increases from 200 nm to 300 nm. PCE is increased till the thickness of $Cs_2AgBiBr_6$ reached 200 nm then it continuously decrease with increase of $Cs_2AgBiBr_6$ width from 200 nm to 300 nm, mainly due to decreased current density. Maximum PCE of 27.87% is obtained at 200 nm thickness of $Cs_2AgBiBr_6$.

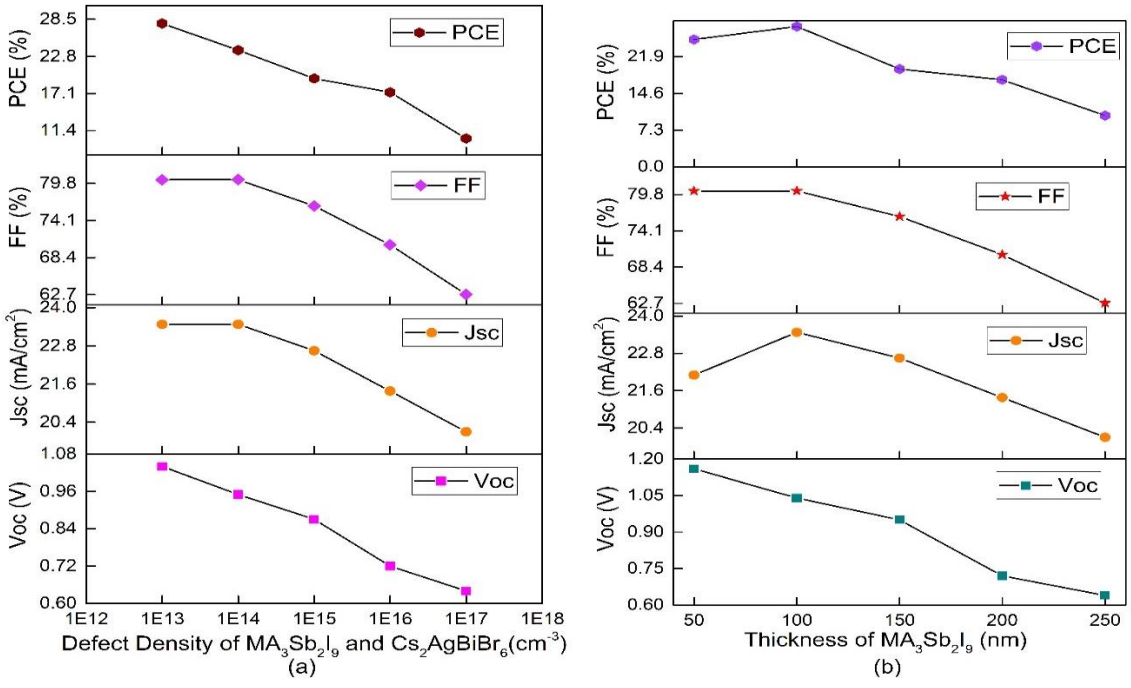

Industrial Engineering Journal
ISSN: 0970-2555
Volume : 52, Issue 11, No. 2, November : 2023

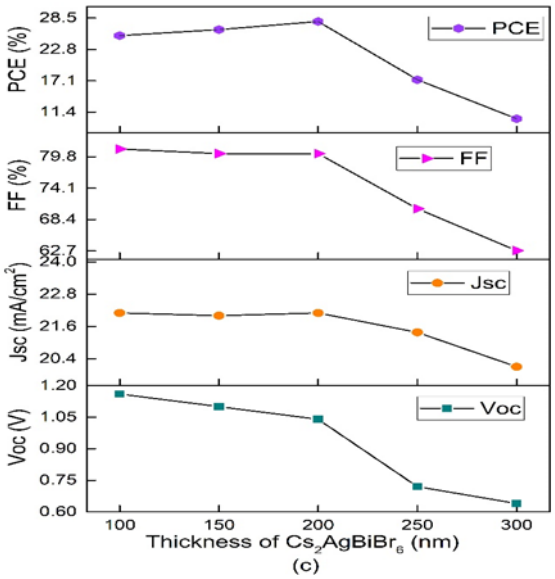

Fig. 3. Shows the solar cell parameters variation with respect to thickness and defect density of PAL.(a) Defect density variation of $MA_3Sb_2I_9$ and $Cs_2AgBiBr_6$ effect on FF , J_{SC} , V_{OC} and PCE .(b) Thickness variation of $MA_3Sb_2I_9$ effect on FF , J_{SC} , V_{OC} and PCE (c) Thickness variation of $Cs_2AgBiBr_6$ effect on FF , J_{SC} , V_{OC} and PCE.

3.2. Impact of variations of Temperature, Shunt Resistance and Series Resistance on PSC parameters

Series resistance is an important parameter in photovoltaic devices, including perovskite solar cells. Series resistance can reduce the fill factor of a solar cell. The fill factor signifies the ability of a solar cell to convert sunlight into electrical power. Increased series resistance can lead to a drop in the fill factor due to losses in the cell's output power. Here the series resistance is varied from 0 Ω cm^2 to 6 Ω cm^2. It is seen that V_{oc} remains constant throughout whereas J_{sc} and FF decreases gradually. PCE first remains constant till the variation of series resistance from 0 Ω cm^2 to 1 Ω cm^2 and then it decreases till series resistance is increased to 6 Ω cm^2. Shunt resistance is another important parameter in the characterization of solar cells. It impacts various key parameters and the overall performance of the solar cell in a manner opposite to that of series resistance. Shunt resistance refers to the resistance pathway in parallel with the photovoltaic cell. Higher shunt resistance contributes positively to the fill factor of solar cells. It helps reduce the leakage current paths, allowing the cell to maintain higher efficiency and output power. Shunt resistance can affect the short-circuit current density. A higher shunt resistance helps minimize the loss of current due to shunting paths, contributing to a higher short-circuit current. Here the shunt resistance is varied from 1×10^1 Ω cm^2 to 1×10^7 Ω cm^2. It is seen that V_{oc} and J_{sc} remains constant throughout whereas FF first remains constant till the variation of shunt resistance from 1×10^1 Ω cm^2 to 1×10^5 Ω cm^2 and then decreases till the variation of shunt resistance from 1×10^5 Ω cm^2 to 1×10^7 Ω cm^2. PCE also first remains constant till the variation of series resistance from 1×10^1 Ω cm^2 to 1×10^6 Ω cm^2 and then it decreases till shunt resistance is increased to 1×10^7 Ω cm^2. Temperature has a major impact on the performance of PSCs, affecting various key parameters in the device. Temperature has direct impact on the open-circuit voltage of PSCs. Generally, as temperature increases, open-circuit voltage decreases. It is due to increased intrinsic carrier concentration and changes in the bandgap of the material at higher temperatures. Temperature also affects the short-circuit current density. An increase in temperature usually leads to a slight increase in the current due to improved carrier mobility and enhanced generation of charge carriers. The FF of perovskite solar cells are influenced by temperature. Higher temperatures often

Industrial Engineering Journal
ISSN: 0970-2555
Volume : 52, Issue 11, No. 2, November : 2023

lead to a decrease in the FF due to increased series resistance and changes in charge carrier recombination rates. The overall PCE of perovskite solar cells are significantly affected by temperature. Here temperature is varied from 275 K to 425 K. J_{sc} remains constant throughout whereas FF, PCE and V_{oc} decrease gradually as the temperature is increased from 275 K to 425 K.

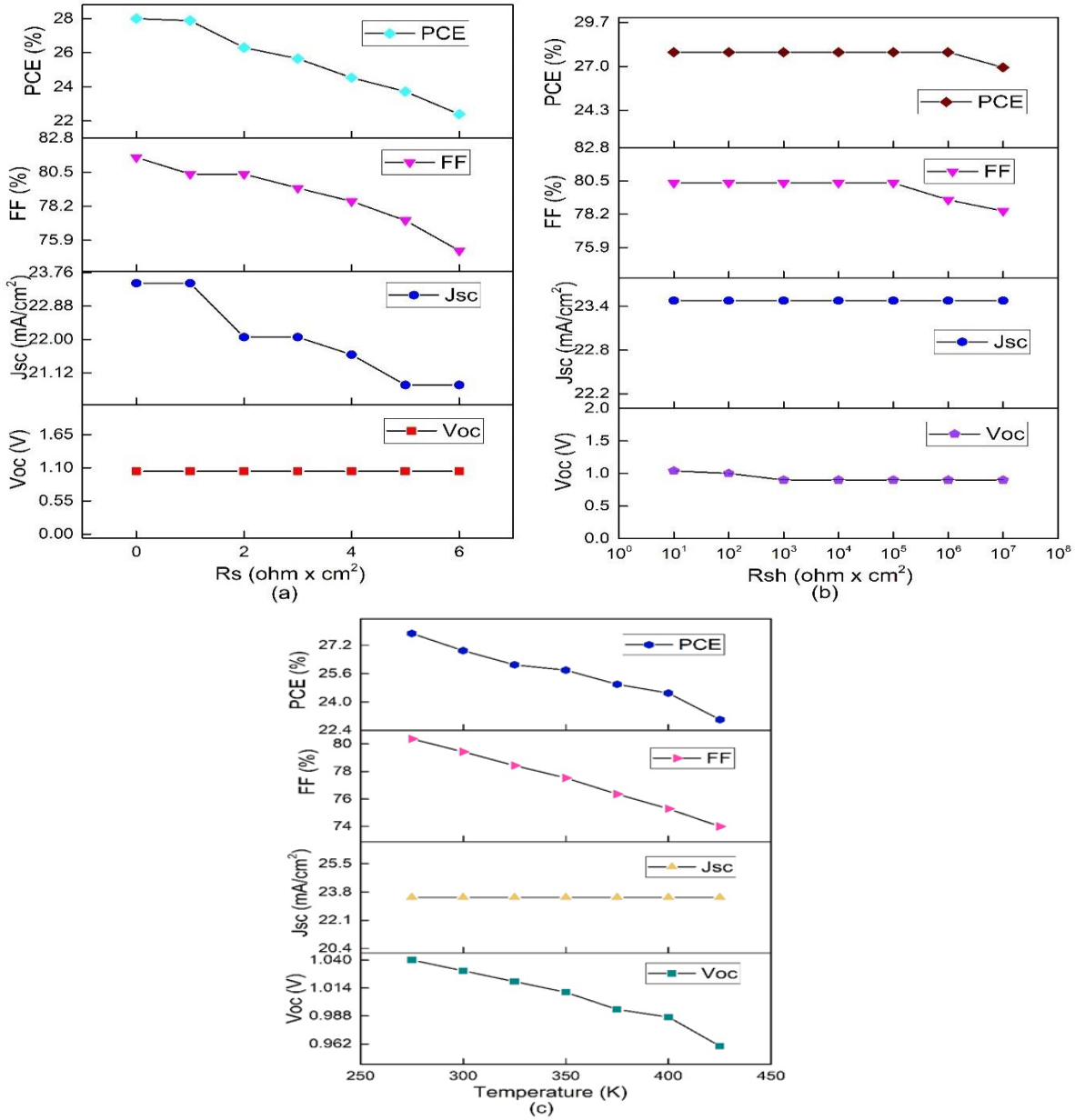

Fig.4. Shows the variation of Solar cell parameters with respect to Temperature, Shunt Resistance and Series Resistance.(a) Series Resistance variation effect on FF , J_{SC} , V_{OC} and PCE.(b) Shunt Resistance variation effect on FF , J_{SC} , V_{OC} and PCE (c) Temperature variation effect on FF , J_{SC} , V_{OC} and PCE.

3.3. VI Characteristics of both N-I-P Structure and P-I-N Structure

Industrial Engineering Journal
ISSN: 0970-2555
Volume : 52, Issue 11, No. 2, November : 2023

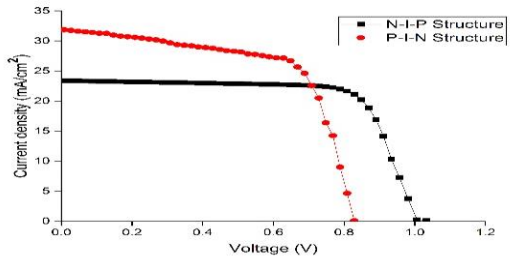

Fig.5. Shows VI Graph of the proposed structure and its inverted structure.

The Voltage-Current (V-I) characteristic of a perovskite solar cell describes relationship between the voltage applied across the solar cell terminals and the resulting current passing through the cell under illumination. It illustrates how the cell behaves electrically and provides important insights into its performance. When a perovskite solar cell is exposed to light, it generates photocurrent due to the absorption of photons and the subsequent creation of electron-hole pairs within the material. The V-I curve under illumination shows the relationship between the voltage and the resulting current in the presence of light. The shape of the V-I curve for a perovskite solar cell may vary based on factors such as the cell's design, material properties, illumination conditions, and temperature. A well-performing perovskite solar cell typically exhibits fill factor, high short-circuit current and high open-circuit voltage approaching unity, leading to a higher efficiency. Here from the above two graphs it is seen that N-I-P Structure is having V_{OC} of 1.04 V which is higher as compared to P-I-N Structure having V_{OC} of 0.818 V. So, we have considered the variation of other parameters of N-I-P Structure as it is having better performance of VI characteristics as compared to the inverted structure.

Table.2. Improvement of PCE over earlier simulated work.

Device Structure	V_{oc} (V)	J_{sc} (mA /cm^2)	FF(%)	PCE(%)	References
PEDOT:PSS/ $MA_3Sb_2I_9$/CdS	1.02	24	81	20.23	[23]
FTO/TiO2/ $Cs_2AgBiBr_6$ /CuI/Au	0.91	23.75	75.23	15.3	[24]
FTO/ TiO2/ $MA_3Sb_2I_9$/Spiro-OMeTAD/Au)	1.0	19.54	82	17.35	[25]
ITO/ZnO/ $Cs_2AgBiBr_6$ /Spiro-OMeTAD/Au	1.52	18.54	69.35	16.3	[26]
Glass/FTO/TiO2/ $Cs_2AgBiBr_6$/Cu2O/Carbon	1.18	22.75	77.73	19.32	[27]
This Work	**1.04**	**23.48**	**80.37**	**27.87**	

4. Conclusions

An extensive investigation has been done for obtaining a high efficiency device configuration of double layered doubly PSC and same has been simulated using SCAPS-1D software. The present study using device structure ITO/TiO_2/$MA_3Sb_2I_9$ /$Cs_2AgBiBr_6$/CuSCN/Au shows a better solar cell parameters, mainly PCE using $MA_3Sb_2I_9$ and $Cs_2AgBiBr_6$ individually for earlier works. Different combinations of width and defect density of PAL has been tried to obtain optimized solar cell parameter. Also the Temperature, Shunt Resistance and Series Resistance effect on the PSC parameters has been studied to use these parameters of optimum value for fabrication of the perovskite solar cell. The simulation of proposed device structure at the thickness of 300 nm and defect density of 1×10^{14} cm^{-3} of PAL, provide best possible power conversion efficiency of 27.87%, Voc of 1.04 V and Jsc of 23.48 mA/cm^2 and FF of 80.37%. This is mainly due to increased charge carrier pairs generation and reduced recombination respectively. It has been found that defect density of PAL is of tremendous effect on improving PCE. The present study will contribute towards the fabrication of highly efficient device of perovskite material $MA_3Sb_2I_9$ and $Cs_2AgBiBr_6$, furthermore reduce dependence on fossil fuel and provide insight to researchers to optimize solar cell parameter in future.

REFERENCES

[1] Mahjabin, Samiya & Haque, Md Mahfuzul & Bin Rafiq, Md Khan & Jamal, M. & Islam, Mohammad & Selvanathan, Vidhya & Assaifan, Abdulaziz & Alharbi, Hamad & Sopian, Kamaruzzaman & Amin, Nowshad & Akhtaruzzaman, Md. (2020). Perceiving of Defect Tolerance in Perovskite Absorber Layer for Efficient Perovskite Solar Cell. IEEE Access. PP. 1-1.

[2] Abdelkader, Hima & Lakhdar, Nacereddine. (2020). Enhancement of efficiency and stability of CH3NH3GeI3 solar cells with CuSbS2. Optical Materials. 99. 109607.

[3] Jani, Md & Islam, Md Tohidul & Al Amin, Syed & Sami, Md & M., Shorowordi & Hossain, Mohammad & Chowdhury, Shaestagir & Nishat, Sadiq & Ahmed, Saquib. (2020). Exploring solar cell performance of inorganic Cs2TiBr6 halide double perovskite: A numerical study. Superlattices and Microstructures. 146. 106652.

[4] Baig, Fasial & Hameed, Yousaf & Ullah, Shafi & Marí Soucase, Bernabé & Beg, Saira & Ullah, Hanif. (2018). Numerical Analysis of a Novel FTO/n-MAPbI 3 /p-MAPbI 3 /p-MAPbBr 3 Organic–Inorganic Lead Halide Perovskite Solar Cell. Journal of Nanoelectronics and Optoelectronics. 13. 1320-1327.

[5] Islam, Md. Aminul & Alamgir, Nabil Bin & Chowdhury, S. & Billah, Baque. (2022). Lead-free organic inorganic halide perovskite solar cell with over 30% efficiency. Journal of Ovonic Research. 18. 395-409.

[6] Bhattarai S, Kalita PK, Hossain I, Alsubaie AS, Mahmoud KH, Ansari MZ, Janicek P. Designing an Efficient Lead-Free Perovskite Solar Cell through a Computational Method. Crystals. 2023

[7] Khac DL, Chowdhury S, Luengchavanon M, Jamal MS, Laref A, Techato K, Sreesawet S, Channumsin S, Chia CH. Influence/Effect of Deep-Level Defect of Absorber Layer and n/i Interface on the Performance of Antimony Triselenide Solar Cells by Numerical Simulation. Sustainability. 2022; 14(11):6780

[8] Nishi Bala, Abhishek Raj, Investigating novel mixed halide Perovskite material $CH_3NH_3Pb(I_{1-x}Cl_x)_3$ to obtain optimized PCE of above 30% in Perovskite Solar Cell, Industrial Engineering Journal, 52, 10 (4), 18-29, 2023.

[9] Shaker, Ahmed & Elsabbagh, Mona & El-Banna, Mohammed. (2018). Impact of nonuniform gate oxide shape on TFET performance: A reliability issue. Physica E Low-dimensional Systems and Nanostructures.

[10] Spampinato C, La Magna P, Valastro S, Smecca E, Arena V, Bongiorno C, Mannino G, Fazio E, Corsaro C, Neri F, et al. Infiltration of CsPbI3:EuI2 Perovskites into TiO2 Spongy Layers Deposited by gig-lox Sputtering Processes. Solar. 2023; 3(3):347-361.

[11] kour, Navneet & Mehra, Dr. Rajesh & Khatana, Chandni. (2018). Efficient design of perovskite solar cell using mixed halide and copper oxide. Chinese Physics B. 27. 018801

[12] Bhat A, Dhamaniya BP, Chhillar P, Korukonda TB, Rawat G, Pathak SK. Analysing the Prospects of Perovskite Solar Cells within the Purview of Recent Scientific Advancements. Crystals. 2018; 8(6):242

[13] Abdulalmohsin, Samir. (2020). Perovskite solar cells based on CH 3 NH 3 SnI 3 Structure. IOP Conference Series: Materials Science and Engineering. 928

[14] Dai X, Koshy P, Sorrell CC, Lim J, Yun JS. Focussed Review of Utilization of Graphene-Based Materials in Electron Transport Layer in Halide Perovskite Solar Cells: Materials-Based Issues. Energies. 2020; 13(23):6335

[15] Omarova Z, Yerezhep D, Aldiyarov A, Tokmoldin N. In Silico Investigation of the Impact of Hole-Transport Layers on the Performance of CH3NH3SnI3 Perovskite Photovoltaic Cells. Crystals. 2022; 12(5):699

[16] Bhattarai S, Mohammed MKA, Madan J, Pandey R, Ansari MZ, Zaki Rashed AN, Amami M, Hossain MK. Performance Improvement of Perovskite Solar Cell Design with Double Active Layer to Achieve an Efficiency of over 31%. Sustainability. 2023; 15(18):13955
[17] S. Mahjabin et al., "Perceiving of Defect Tolerance in Perovskite Absorber Layer for Efficient Perovskite Solar Cell," in IEEE Access, vol. 8, pp. 106346-106353, 2020.
[18] F. Zhang, B. Yang, Y. Li, W. Deng, and R. He, ‘‘Extra long electron–hole diffusion lengths in CH3NH3PbI3 x Clx perovskite sin- gle crystals,’’ J. Mater. Chem. C, vol. 5, no. 33, pp. 8431–8435, 2017.
[19] H.-S. Kim, C.-R. Lee, J.-H. Im, K.-B. Lee, T. Moehl, A. Marchioro, S.-J. Moon, R. Humphry-Baker, J.-H. Yum, J. E. Moser, M. Grätzel, and N.-G. Park, ‘‘Lead iodide perovskite sensitized all-solid-state submicron thin film mesoscopic solar cell with efficiency exceeding 9%,’’ Sci. Rep., vol. 2, no. 1, Dec. 2012, Art. no. 591.
[20] W. S. Yang, B.-W. Park, E. H. Jung, N. J. Jeon, Y. C. Kim, D. U. Lee, S. S. Shin, J. Seo, E. K. Kim, J. H. Noh, and S. I. Seok, ‘‘Iodide manage- ment in formamidinium-lead-halide–based perovskite layers for efficient solar cells,’’ Science, vol. 356, no. 6345, pp. 1376–1379, 2017.
[21] N. Torabi et al., “Development of a silver/polymer nanocomposite interconnection layer for organic tandem solar cells,” J. Nanophotonics 9, 093049 (2015).
[22] M.M. Tavakoli, P. Yadav, R. Tavakoli, J. Kong, Surface engineering of TiO2 ETL for highly efficient and hysteresis-less planar perovskite solar cell (21.4%) with enhanced open-circuit voltage and stability, Adv. Energy Mater. 8 (2018) 1–9, https://doi.org/10.1002/aenm.201800794.
[23] A. Buin, R. Comin, J. Xu, A.H. Ip, E.H. Sargent, “ Halide-dependent electronic structure of organolead perovskite materials,” Chem. Mater. 27 (2015) 4405–4412.
[24] P. Docampo, F.C. Hanusch, S.D. Stranks, M. Doblinger, € J.M. Feckl, M. Ehrensperger, N.K. Minar, M.B. Johnston, H.J. Snaith, T. Bein, “Deposition-conversion for planar heterojunction mixed halide perovskite solar cells,” Adv. Energy Mater. 4 (2014) 1–6, https://doi.org/10.1002/
[25] M. S. Salem Basyoni et al.: On Investigation of Interface Defects of Solar Cells, IEEE Access , vol. 9,2021 doi :10.1109/ACCESS.2021.3114383
[26] M Ayad, M Fathi, A Mellit, ‘‘Study and performance analysis of Perovskite solar cell structure based on organic and inorganic thin films,’’ Optik, vol. 233, May 2021, Art. no. 166619.
[27] Shambhavi Rai, B.K. Pandey, D.K. Dwivedi., “Modeling of highly efficient and low cost CH3NH3Pb(I1-xClx)3based perovskite solar cell by numerical simulation,” Optical Materials, Volume 100, February 2020, Art no.109631